JACS
JOURNAL OF THE AMERICAN CHEMICAL SOCIETY

COMMUNICATION

pubs.acs.org/JACS

On the Reactivity of Mononuclear Iron(V)oxo Complexes

Soumen Kundu, Jasper Van Kirk Thompson, Alexander D. Ryabov,* and Terrence J. Collins*

Department of Chemistry, Carnegie Mellon University, 4400 Fifth Avenue, Pittsburgh, Pennsylvania 15213, United States

Supporting Information

ABSTRACT: Ferric tetraamido macrocyclic ligand (TAML)-based catalysts [Fe{C_6H_4-1,2-($NCOCMe_2NCO)_2CR_2$}-(OH_2)]PPh_4 [**1**; R = Me (**a**), Et (**b**)] are oxidized by *m*-chloroperoxybenzoic acid at −40 °C in acetonitrile containing trace water in two steps to form Fe(V)oxo complexes (**2a**,**b**). These uniquely authenticated $Fe^V(O)$ species comproportionate with the Fe^{III} starting materials **1a**,**b** to give μ-oxo-$(Fe^{IV})_2$ dimers. The comproportionation of **1a**−**2a** is faster and that of **1b**−**2b** is slower than the oxidation by **2a**,**b** of sulfides (*p*-XC_6H_4SMe) to sulfoxides, highlighting a remarkable steric control of the dynamics. Sulfide oxidation follows saturation kinetics in [*p*-XC_6H_4SMe] with electron-rich substrates (X = Me, H), but changes to linear kinetics with electron-poor substrates (X = Cl, CN) as the sulfide affinity for iron decreases. As the sulfide becomes less basic, the Fe^{IV}/Fe^{III} ratio at the end of reaction for **2b** suggests a decreasing contribution of concerted oxygen-atom transfer ($Fe^V \rightarrow Fe^{III}$) concomitant with increasing electron transfer oxidation ($Fe^V \rightarrow Fe^{IV}$). Fe^V is more reactive toward PhSMe than Fe^{IV} by 4 orders of magnitude, a gap even larger than that known for peroxidase Compounds I and II. The findings reinforce prior work typecasting TAML activators as faithful peroxidase mimics.

High-valent iron−oxo complexes are key reactive intermediates in numerous biochemical oxidations. The most oxidized are commonly isoelectronic with Fe(V) having one oxidation equivalent residing on porphyrin and the second on Fe(IV). While there is a substantial literature of well-characterized Fe^{IV}oxo species,[1] $Fe^V(O)$ reactive intermediates have rarely been proposed. Examples include the Rieske dioxygenase enzyme[2] and certain non-heme iron biomimetic systems.[3] In the tetraamido macrocyclic ligand (TAML) environment, however, $Fe^V(O)$ has been trapped and authenticated via spectroscopic, structural, and theoretical studies.[4] Iron(IV)oxo[5] and μ-oxo-$(Fe^{IV})_2$[5,6] TAML species also have been well-characterized. For multiple reasons, it is important to examine mechanistically the reactivity of these authentic $Fe^V(O)$ complexes. First, as Collman and colleagues have pointed out, "Only by associating particular complexes with the kinetic behavior of the catalytic reaction can one be certain that this complex is contributing to the catalytic process,"[7] a challenge that has been encountered and discussed previously in biomimetic oxidation chemistry.[8] Second, $Fe^V(O)$ reactivities must be compared with those of the corresponding Fe^{IV} species to assess the relative and collaborative roles in catalysis. Third, the rates of $Fe^V(O)$ reactions with other iron complexes in the catalytic medium should be measured to learn how such processes might modulate the catalysis. Herein we describe these reactivity features for **2a**,**b**, the $Fe^V(O)$ complexes[4] by studying the oxidations of aryl methyl sulfides (ArSMe) to sulfoxides. We show that **2a**,**b** can serve as kinetically competent reactive intermediates in peroxidase-like catalysis and the reactivity depends strongly upon subtle steric effects in the macrocyclic ligand.

Scheme 1. Starting Ferric Complexes (1) and the Interconversions of Fe^{III}, Fe^{IV}, and Fe^V Species at −40 °C in MeCN Containing 0.2% (v/v) H_2O

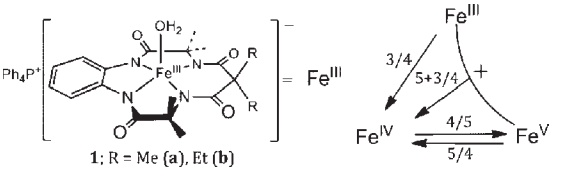

1; R = Me (**a**), Et (**b**)

Complex **2a** was prepared at −40 °C from **1a** in MeCN containing 0.2% (v/v) H_2O by adding *m*-chloroperoxybenzoic acid (*m*CPBA).[4] The starting **1a** (2.0×10^{-4} M) reacted with 0.5 equiv of *m*CPBA (1.0×10^{-4} M) to give the μ-oxo-$(Fe^{IV})_2$ dimer (Figure 1A). A second 0.5 equiv of *m*CPBA (1.0×10^{-4} M) converted the μ-oxo-$(Fe^{IV})_2$ dimer to **2a** (Figure 1B). The $Fe^{III} \rightarrow Fe^{IV}$ conversion ($k_{3/4}$) is ca. 10 times faster than the $Fe^{IV} \rightarrow Fe^V$ transformation ($k_{4/5}$) (Table 1), where $k_{3/4}$ is the effective second-order rate constant at low [*m*CPBA] [Figure 1S in the Supporting Information (SI)] and $k_{4/5}$ was measured directly at [Fe^{IV}] = [*m*CPBA] (Figure 2S). On the basis of the extinction coefficient reported (and supported by Mössbauer quantification),[4] the amount of **2a** formed was not less than 95% of the total iron. Prior to measurements of the rates of oxidation by **2** of the sulfide series *p*-XC_6H_4SMe, potentially interfering interactions among Fe^{III}, Fe^{IV}, and Fe^V (Scheme 1) were investigated kinetically.

First, $Fe^V(O)$ converts to Fe^{IV} in MeCN. This process is much slower than the reduction of $Fe^V(O)$ by ArSMe. Therefore, it is not an interfering reaction. The decay is first-order in Fe^V (Figure 3S), and the first-order rate constants $k_{5/4}$ are given in Table 1. Significantly, the decay of Fe^V to Fe^{IV} ($k_{5/4}$) is 10 times faster for **2b** than for **2a** (Table 1), in agreement with the macrocyclic ligand C−H cleavage mechanism proposed elsewhere.[9]

Second, both the formation of $Fe^V(O)$ and the comproportionation with Fe^{III} ($k_{5+3/4}$) have been postulated to occur in water above 0 °C, where $Fe^V(O)$ is thought to have a fleeting existence.[10] Since comproportionation between **2** and **1** formed upon substrate oxidation would tame the behavior of $Fe^V(O)$

Received: August 24, 2011
Published: October 10, 2011

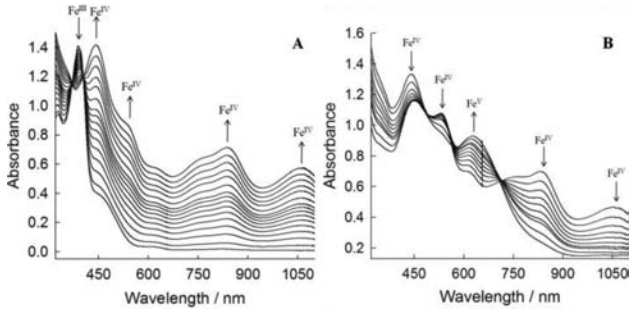

Figure 1. Spectral changes for the (A) $Fe^{III} \rightarrow Fe^{IV}$ and (B) $Fe^{IV} \rightarrow Fe^{V}$ conversions. Conditions: [**1a**] = 2×10^{-4} M; [*m*CPBA] = $(1 + 1) \times 10^{-4}$ M [added in two steps for the sequential conversions in (A) and (B)]; [H_2O] = 0.2% (v/v); MeCN; −40 °C. Figure 6S shows similar spectral changes with **1b**.

Table 1. Rate Constants ($k_{5/4}$ in s^{-1}, All Others in M^{-1} s^{-1}) for the Interconversions between Fe^{III}, Fe^{IV}, and Fe^{V} Species (Scheme *1*) in the Absence of Sulfide at −40 °C in MeCN Containing 0.2% (v/v) H_2O

complex	$k_{3/4}$[a]	$k_{4/5}$[b]	$k_{5/4}$	$k_{5+3/4}$
1a (R = Me)	280 ± 20	18 ± 1	$(1.0 \pm 0.1) \times 10^{-5}$	$(4 \pm 1) \times 10^{4}$
1b (R = Et)	800 ± 100	47 ± 3	$(1.11 \pm 0.02) \times 10^{-4}$	35 ± 1

[a] $k_{3/4} = kK$, as calculated from the established rate law: $v = kK[Fe^{III}]_t[m\text{CPBA}]/(1 + K[m\text{CPBA}])$. [b] Measured directly at $[Fe^{IV}] = [m\text{CPBA}]$ (see the SI for details).

toward the remaining substrate, it was important to measure $k_{5+3/4}$ as we did here in MeCN to evaluate potential moderating effects on the catalysis. When an equimolar amount of Fe^{III} was added to a solution of freshly prepared $Fe^{V}(O)$ at −40 °C, comproportionation led quantitatively to μ-oxo-$(Fe^{IV})_2$ (Figures 4S and 5S). Studies of **2a**,**b** revealed that this rate is under ligand control. The comproportionation of **2b** and **1b** is 10^3 times slower than that of **2a** and **1a** (Table 1), yet **2a** and **2b** are similar electronically. Thus, we attribute the large difference in $k_{5+3/4}$ to the bulkier ethyl (**2b**) versus methyl (**2a**) groups on each face of the macrocycle that hinder the formation of μ-oxo-$(Fe^{IV})_2$. We conclude that steric effects should be explored through TAML activator design to control the selectivity. In porphyrin chemistry, it is well-known that steric effects can influence comproportionations.[11]

Having observed and quantified the rates of processes relating Fe^{V}, Fe^{IV}, and Fe^{III} in the absence of a substrate, we next studied the oxidations of ArSMe by **2**. At [**2**] = 2×10^{-4} M (used to produce Figure 1), the ArSMe oxidations were too fast for conventional UV−vis techniques. Therefore, **2** was used at a lower concentration (5×10^{-5} M), where excess *m*CPBA (1×10^{-4} M, 2 equiv) was required for quantitative conversion of **1** to **2**. On the time scales of the sulfide oxidations under the conditions employed, this excess *m*CPBA did not react with either ArSMe or **1** fast enough to affect the kinetic behavior (see the SI).

Oxidations of organic sulfides to sulfoxides by biological and biomimetic catalysts are known to proceed by both oxygen-atom transfer (OT) and electron transfer (ET) mechanisms, suggesting that either process or both could be found here.[12] The $Fe^{V}(O)$ oxidations of sulfides were assayed at the isosbestic points for Fe^{III} and Fe^{IV} interconversions (370 and 375 nm for **2a**,**b**, respectively; Figure 1 and Figures 6SA,B). The isosbestic

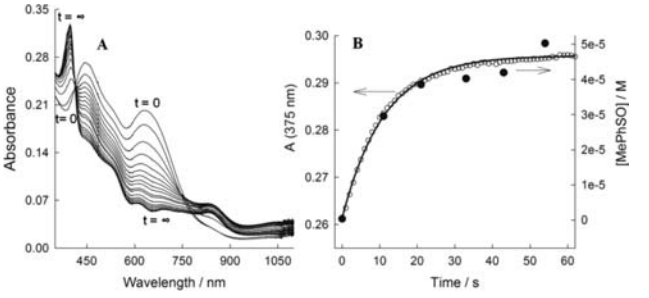

Figure 2. (A) UV−vis changes for **2b** (5×10^{-5} M) reduction by PhSMe (5×10^{-4} M). (B) Absorbance at 375 nm (○) and the amount of PhMeSO formed (●) measured by HPLC; see the SI) vs time under the same conditions. The solid line was calculated using $k_{obs} = 0.084\ s^{-1}$. Conditions: −40 °C, 0.2% (v/v) H_2O/MeCN.

points held even in excess ArSMe (Figure 7S). On addition of at least a 10-fold excess of PhSMe (chosen for the most extensive studies), the UV−vis absorbances at 370 nm (**2a**) or 375 nm (**2b**) rapidly increased. The full spectra indicated that **2a** was converted to Fe^{IV} quantitatively (Figure 8S) and that **2b** produced a mixture of Fe^{III} and Fe^{IV} (Figure 2A). This difference results from the divergent comproportionation rates (see below). Figure 2B shows the matching kinetics of the reduction of **2b** and the formation of PhMeSO (HPLC analysis; see the SI). At the end of the reactions, PhMeSO was produced quantitatively (HPLC and GC−MS analysis for both the **2a** and **2b** processes), even though considerable Fe^{IV} remained at the end of the process in each case. The reaction of Fe^{IV} with PhSMe is slow under the experimental conditions (see below). Analyses of PhSMe/PhMeSO were performed at room temperature after quenching with the more reactive *p*-$MeOC_6H_4SMe$. Two-electron reduction of Fe^{V} to Fe^{III} by PhSMe should produce equivalent amounts of Fe^{III} and sulfoxide. One-electron reduction of Fe^{V} to Fe^{IV} should first produce the corresponding intermediate cation radical $ArMeS^{\bullet+}$.[13] In water, $ArMeS^{\bullet+}$ is known to react with O_2 to form sulfoxide, where the oxygen in sulfoxide originates from water and not from O_2.[14] Thus, a consistent explanation for the observed stoichiometry is that $ArMeS^{\bullet+}$, produced in an Fe^{V} to Fe^{IV} step, is swept on rapidly by O_2 to ArMeSO, leaving residual Fe^{IV} while giving one sulfoxide for each $Fe^{V} \rightarrow Fe^{IV}$ event. Attempts to observe $ArMeS^{\bullet+}$ or the peroxyl radical $ArMeSO_2^{\bullet+}$ by EPR spectroscopy were unsuccessful (see the SI). This does not rule out these putative intermediates but mandates that further reactions to sulfoxide be fast if these are indeed formed. Oxidation of PhSMe by $Fe^{V}O$ in the presence of $H_2{}^{18}O$ gave 25% incorporation of ^{18}O in the product PhMeSO.[4] Both the OT (via fast oxo ligand exchange) and ET[14] pathways can lead to labeled PhMeSO.

The absorbance-versus-time traces for reduction of **2a**,**b** are exponential, indicating first-order kinetics in **2a**,**b**, which holds for at least four half-lives. Thus, presumptive conversion of $ArMeS^{\bullet+}$ to ArMeSO by O_2 does not intrude into the kinetic analysis of $Fe^{V}(O)$ reactions. The reactions of $Fe^{V}(O)$ with *p*-XC_6H_4SMe [X = Me (**2b**); H, Cl, CN (**2a**,**b**)] were measured under pseudo-first-order conditions in excess of sulfide. With X = MeO (**2a**,**b**) and Me (**2a**), the processes were too fast for pseudo-first-order treatment, so another approach was used for the kinetic analysis (see below). The values of k_{obs} for the reduction of $Fe^{V}(O)$ by ArSMe were collected in excess sulfide at concentrations of $(0.5-4.2) \times 10^{-3}$ M (Figure 3A for **2b** and Figure 10SA for **2a**).

dx.doi.org/10.1021/ja208007w | *J. Am. Chem. Soc.* 2011, 133, 18546–18549

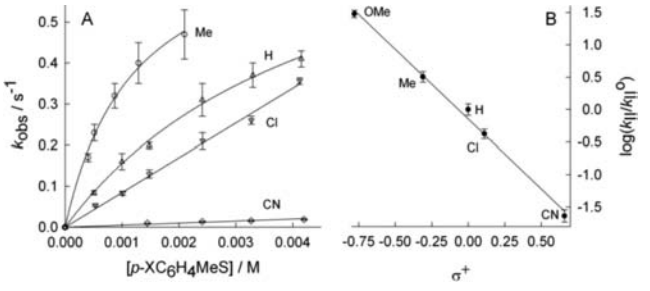

Figure 3. (A) Pseudo-first-order rate constants k_{obs} plotted against the [*p*-XC$_6$H$_4$SMe]. Conditions: [**2b**] = 5×10^{-5} M; [H$_2$O] = 0.2% (v/v); −40 °C in MeCN. (B) Hammett plot for k_{II} vs σ^+ (see the text for details). Figure 10S shows similar plots for **2a**.

Scheme 2. Proposed Reaction Mechanism

$$Fe^{V}O + ArSMe \underset{}{\overset{K_1}{\rightleftharpoons}} \{ArSMe,Fe^{V}O\}$$

$$Fe^{V}O + ArSMe \xrightarrow{k_{II}} Fe^{III/IV} + ArMeSO/\dot{A}rS\dot{M}e$$

$$Ar\diagdown S\text{–}Fe^{v}=O = \{ArSMe,Fe^{V}O\} \text{ or } \boldsymbol{I}$$

For **2a,b**, the k_{obs} values show similar trends, but **2a** is 2−6 times more reactive than **2b**, suggesting that Me-versus-Et steric effects are again significant.

Over the concentration range in Figure 3, the k_{obs} dependencies on [ArSMe] are hyperbolic for electron-rich and linear for electron-poor sulfides for both **2a,b**. Nevertheless, this behavioral diversity is consistent with a common rate law: $k_{obs} = k_{II}[ArSMe]/(1 + K_1[ArSMe])$ eq 1 provided that $K_1[ArSMe] \ll 1$ for sulfides with X = Cl, CN. This was confirmed by measuring k_{obs} for **2a** with *p*-NCC$_6$H$_4$SMe at higher [ArSMe] [$(0.5-5) \times 10^{-2}$ M], where saturation kinetics emerged. The rate law requires the reversible formation of an Fe^V(O)−sulfide adduct, such as ***I*** (Scheme 2). PhMeSO (5×10^{-5} M) did not inhibit the oxidation of PhSMe (5×10^{-4} and 2×10^{-3} M) by **2a** or **2b** (5×10^{-5} M), showing that the sulfoxide product does not bind to Fe^{V}O under the reaction conditions.

Because reactions of *p*-XC$_6$H$_4$SMe [X = OMe (**2a,b**), Me (**2a**)] were too fast for pseudo-first-order treatment, k_{II} was determined at [Fe^V(O)] = [ArSMe] = 5×10^{-5} M assuming second-order kinetics (**2b**; Figure 9S). It is realistic because for the most electronically similar sulfide, *p*-MeC$_6$H$_4$SMe, at [ArSMe] = 5×10^{-5} M with K_1(**2b**) ≈ 10^3 M^{-1}, eq 1 becomes $k_{obs}/[ArSMe] \approx k_{II}$. The k_{II} values were obtained by fitting the data to the equation $A_t = A_0 + (a_0^2 k_{II} \Delta\varepsilon t)/(1 + a_0 k_{II} t)$, where $\Delta\varepsilon$ is the extinction coefficient difference of the Fe^{III} and Fe^V species and A_0 and A_t are the absorbances at times 0 and t, respectively (see the SI). k_{II} for X = OMe (Table 2) is comparable to that for oxidation of SMe$_2$ by (*meso*-Mes$_4$porphyrin$^{+\bullet}$)Fe^{IV}oxo under similar conditions.[15]

In the case of **2b**, where comproportionation is slow, the UV−vis spectra show that both Fe^{III} and Fe^{IV} are generated by sulfide. This implies that k_{obs} reflects a summation of the rates for the parallel reductions of Fe^V(O) to Fe^{III} (OT pathway) and/or of Fe^V(O) to Fe^{IV} (ET pathway),[16] i.e., $k_{obs} = k_{obs}^{OT} + k_{obs}^{ET}$ and $k_{obs}^{OT}/k_{obs}^{ET}$ = [Fe^{III}]/[Fe^{IV}]. $k_{obs}^{OT}/k_{obs}^{ET}$ could be determined for **2b** but not for **2a** (fast comproportionation). The relative contributions of the OT and ET pathways for **2b** were calculated from the absorbance at 722 nm, where the molar absorptivities of Fe^V and Fe^{IV} are the same but Fe^{III} does not absorb (Figure 6SB). When the Fe^V conversion is 95%, the absorbance at 722 nm is given by

Table 2. Rate and Equilibrium Constants for the Oxidations of *p*-XC$_6$H$_4$SMe by Fe^V(O) and Relative Contributions of the OT and ET Pathways, $k_{obs}^{OT}/k_{obs}^{ET}$, for 2b[a]

	2b (R = Et)			**2a** (R = Me)	
X	K_1/M^{-1}	k_{II}/M^{-1} s^{-1}	$k_{obs}^{OT}/k_{obs}^{ET}$[b]	K_1/M^{-1}	k_{II}/M^{-1} s^{-1}
MeO		5000 ± 400			9000 ± 700
Me	800 ± 100	600 ± 80	1.9 ± 0.1		3900 ± 250
H	210 ± 30	190 ± 30	0.88 ± 0.07	500 ± 50	450 ± 50
Cl		80 ± 2	0.57 ± 0.09		165 ± 5
CN		4.4 ± 0.5	0.20 ± 0.01	23 ± 4[c]	13 ± 5[c]
					11.5 ± 0.5

[a] See the text for details. Conditions: −40 °C in 0.2% (v/v) H$_2$O/MeCN. [b] Calculated at the time of 95% conversion of Fe^V(O) at [ArSMe] = 5×10^{-4} M. [c] Obtained using 0.005−0.05 M *p*-NCC$_6$H$_4$SMe.

$0.05[Fe]_t\varepsilon_V + [Fe^{IV}]\varepsilon_{IV}$, so $[Fe^{III}]/[Fe^{IV}] = (\varepsilon_{IV}[Fe]_t - A_{722})/(A_{722} - 0.05[Fe]_t\varepsilon_{IV})$. The time at which A_{722} should be read was calculated from k_{obs} for each sulfide at [*p*-XC$_6$H$_4$SMe] = 5×10^{-4} M. The [Fe^{III}]/[Fe^{IV}] ratios (=$k_{obs}^{OT}/k_{obs}^{ET}$) are included in Table 2. These ratios indicate that (i) the ET pathway is favored for the electron-poor sulfides, and (ii) the OT pathway is favored for the electron-rich sulfides. Hammett plots were made for both **2a,b**. The fit for **2b** (Figure 3B) improved when $\log(k_{II}/k_{II}^o)$ values were plotted against σ^+ constants[17] ($\rho^+ = -2.15 \pm 0.09$, $r^2 = 0.994$) instead of σ ($\rho = -3.0 \pm 0.4$, $r^2 = 0.939$), suggesting that resonance effects are significant. For **2a**, the plot of $\log(k_{II}/k_{II}^o)$ versus σ^+ (Figure 10SB) had a similar slope of -2.1 ± 0.3 (ρ^+). Thus, the electrophilicities of **2a,b** are similar, supporting the idea that steric effects result in different comproportionation rates. The absolute ρ values are larger than those for the oxidation of organic sulfides to sulfoxides by reconstituted cytochrome P450 ($\rho^+ = -0.16$, σ^+),[18] (salen$^{+\bullet}$)-Fe(IV)oxo complexes ($\rho = -0.65$ to -1.54, σ),[19] or a mononuclear non-heme Fe(IV)oxo complex ($\rho = -1.0$, σ_p).[20] This suggests that the sulfide X substituent is in strongest electronic communication with the reactive center in the **2a,b** case. To obey the rate law, ***I*** cannot react with another sulfide and be involved in the bimolecular OT pathway, as this would require a higher kinetic order in sulfide. The geometric constraints appear to forbid intramolecular OT through ***I*** (Scheme 2). Also to obey the rate law, the ET pathway could proceed either through a bimolecular step involving uncoordinated Fe^{V}O and sulfide (Scheme 2), with ***I*** forming in an unproductive equilibrium, or via homolysis of the Fe−S bond in ***I***. Both processes can deliver the observed saturation kinetics of k_{obs} on [ArSMe]. The kinetic data presented cannot distinguish between the two cases. It has been proposed that (salen$^{+\bullet}$)Fe(IV)oxo complexes bind sulfides reversibly at the oxo ligand,[19] which would represent another way to produce saturation kinetics. However, we find it hard to imagine that this process could be reversible: once the sulfur has approached the oxo ligand at the van der Waals distance or less, the electronic reorganization required to make the sulfoxide would occur instantaneously, at which point the reaction would be over.

Having studied how Fe^{V}O interacts with sulfides, we concluded by examining the comparative behavior of Fe^{IV} with PhSMe. The reactivity of the μ-oxo-(Fe^{IV})$_2$ dimer was quantified by measuring at 750 nm the initial rates of its reaction with PhSMe (Figure 4) to form Fe^{III} and PhMeSO (Figure 7S). The

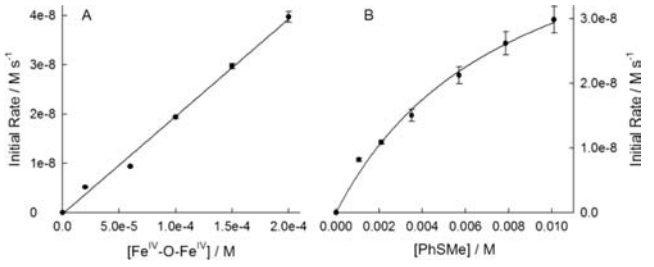

Figure 4. Kinetics of reduction of Fe^{IV} to Fe^{III} by PhSMe. (A) Initial rate of reduction of Fe^{IV} as a function of $[Fe^{IV}]$. Conditions: [PhSMe] = 2.1×10^{-3} M, 0.2% (v/v) H_2O/MeCN, −40 °C. (B) Initial rate of reduction of Fe^{IV} as a function of [PhSMe]. Conditions: $[Fe^{IV}] = 1 \times 10^{-4}$ M, 0.2% (v/v) H_2O/MeCN, −40 °C.

initial rate varied linearly with $[Fe^{IV}]$ and exhibited saturation kinetics with [PhSMe] (Figure 4), suggesting the reversible formation of a sulfide adduct. The data were fitted to the rate equation $v = k_{4/3}[Fe^{IV}][PhSMe]/(1 + K[PhSMe])$ to obtain the values $K = (120 \pm 25)\ M^{-1}$ and $k_{4/3} = (6 \pm 1) \times 10^{-2}\ M^{-1}\ s^{-1}$, where $k_{4/3}$ corresponds to the rate constant characterizing the reactivity of Fe^{IV}. The oxidant $Fe^{V}(O)$ is more reactive than this Fe^{IV} species by 4 orders of magnitude, a gap even larger than that known for Compounds I and II of horseradish peroxidase.[21]

In conclusion, the first detailed reactivity studies of authentic Fe(V)oxo complexes have revealed rapid sulfide oxidations. The $Fe^{V}(O)$ reagents form from Fe^{III} via Fe^{IV}, where comproportionation might be involved. $Fe^{V}(O)$ is 4 orders of magnitude more reactive toward sulfides than Fe^{IV}. This suggests that the $Fe^{V}(O)$ species have the high reactivity needed for catalytic oxidations.[22] Among the potentially intruding degradation and comproportionation reactions of the $Fe^{V}(O)$ reagent, only the latter is active under the conditions employed. The $Fe^{V}(O)$ engages in oxygen-atom transfer with organic sulfides, establishing an $Fe^{V} \rightarrow Fe^{III}$ redox process. Nevertheless, despite high rates of formation of sulfoxides from sulfides at low temperature, the OT dominates only slightly over ET and then only for the electron-rich sulfides in the studied ArSMe series. Electron-withdrawing groups induce the sulfides to react predominantly via ET. The comproportionation between Fe^{V} and Fe^{III} is very sensitive to steric effects and is strongly hindered by the relatively minor exchange of a methyl for an ethyl substituent. Steric effects also slow the reactions of sulfides with **2b** relative to **2a**. This points to a large scope for designing steric effects into TAML systems to control the selectivity in oxidation catalysis.

■ ASSOCIATED CONTENT

Supporting Information. Experimental details and kinetic measurements. This material is available free of charge via the Internet at http://pubs.acs.org.

■ AUTHOR INFORMATION

Corresponding Author
tc1u@andrew.cmu.edu; ryabov@andrew.cmu.edu.

■ ACKNOWLEDGMENT

Support from the Heinz Endowments, the Institute for Green Science and CMU is acknowledged (T.J.C). We thank Dr. Deboshri Banerjee for preliminary measurements and Rupal Gupta for EPR assistance. S.K. thanks the R. K. Mellon Foundation for a Presidential Fellowship in the Life Sciences. J.V.K.T. thanks CMU for a Small Undergraduate Research Grant.

■ REFERENCES

(1) (a) Costas, M.; Mehn, M. P.; Jensen, M. P.; Que, L., Jr. *Chem. Rev.* **2004**, *104*, 939. (b) Kryatov, S. V.; Rybak-Akimova, E. V.; Schindler, S. *Chem. Rev.* **2005**, *105*, 2175. (c) Pestovsky, O.; Stoian, S.; Bominaar, E. L.; Shan, X.; Münck, E.; Que, L., Jr.; Bakac, A. *Angew. Chem., Int. Ed.* **2005**, *44*, 6871. (d) Meunier, B. *Models of Heme Peroxidases and Catalases*; Imperial College Press: London, 2000.

(2) Shan, X.; Que, L., Jr. *J. Inorg. Biochem.* **2006**, *100*, 421.

(3) (a) Das, P.; Que, L., Jr. *Inorg. Chem.* **2010**, *49*, 9479. (b) Prat, I.; Mathieson, J. S.; Güell, M.; Ribas, X.; Luis, J. M.; Cronin, L.; Costas, M. *Nat. Chem.* **2011**, *3*, 788. (c) Company, A.; Gómez, L.; Güell, M.; Ribas, X.; Luis, J. M.; Que, L., Jr.; Costas, M. *J. Am. Chem. Soc.* **2007**, *129*, 15766. (d) Harischandra, D. N.; Zhang, R.; Newcomb, M. *J. Am. Chem. Soc.* **2005**, *127*, 13776.

(4) Tiago de Oliveira, F.; Chanda, A.; Banerjee, D.; Shan, X.; Mondal, S.; Que, L., Jr.; Bominaar, E. L.; Münck, E.; Collins, T. J. *Science* **2007**, *315*, 835.

(5) Chanda, A.; Shan, X.; Chakrabarti, M.; Ellis, W. C.; Popescu, D. L.; Tiago de Oliveira, F.; Wang, D.; Que, L., Jr.; Collins, T. J.; Münck, E.; Bominaar, E. L. *Inorg. Chem.* **2008**, *47*, 3669.

(6) Ghosh, A.; Tiago de Oliveira, F.; Yano, T.; Nishioka, T.; Beach, E. S.; Kinoshita, I.; Münck, E.; Ryabov, A. D.; Horwitz, C. P.; Collins, T. J. *J. Am. Chem. Soc.* **2005**, *127*, 2505.

(7) Collman, J. P.; Hegedus, L. S.; Norton, J. R.; Finke, R. G. *Principles and Applications of Organotransition Metal Chemistry*; University Science Books: Mill Valley, CA, 1987.

(8) (a) Lyakin, O. Y.; Bryliakov, K. P.; Britovsek, G. J. P.; Talsi, E. P. *J. Am. Chem. Soc.* **2009**, *131*, 10798. (b) Chen, K.; Costas, M.; Kim, J.; Tipton, A. K.; Que, L., Jr. *J. Am. Chem. Soc.* **2002**, *124*, 3026.

(9) Bartos, M. J.; Gordon-Wylie, S. W.; Fox, B. G.; Wright, L. J.; Weintraub, S. T.; Kauffmann, K. E.; Münck, E.; Kostka, K. L.; Uffelman, E. S.; Rickard, C. E. F.; Noon, K. R.; Collins, T. J. *Coord. Chem. Rev.* **1998**, *174*, 361.

(10) (a) Ghosh, A.; Mitchell, D. A.; Chanda, A.; Ryabov, A. D.; Popescu, D. L.; Upham, E.; Collins, G. J.; Collins, T. J. *J. Am. Chem. Soc.* **2008**, *130*, 15116. (b) Popescu, D.-L.; Vrabel, M.; Brausam, A.; Madsen, P.; Lente, G.; Fabian, I.; Ryabov, A. D.; van Eldik, R.; Collins, T. J. *Inorg. Chem.* **2010**, *49*, 11439.

(11) Collman, J. P.; Gagne, R. R.; Reed, C. A.; Halbert, T. R.; Lang, G.; Robinson, W. T. *J. Am. Chem. Soc.* **1975**, *97*, 1427.

(12) Goto, Y.; Matsui, T.; Ozaki, S.-i.; Watanabe, Y.; Fukuzumi, S. *J. Am. Chem. Soc.* **1999**, *121*, 9497.

(13) Kobayashi, S.; Nakano, M.; Kimura, T.; Schaap, A. P. *Biochemistry* **1987**, *26*, 5019.

(14) (a) Schöneich, C.; Aced, A.; Asmus, K.-D. *J. Am. Chem. Soc.* **1993**, *115*, 11376. (b) Bonifačić, M.; Hug, G. L.; Schöneich, C. *J. Phys. Chem. A* **2000**, *104*, 1240.

(15) Franke, A.; Fertinger, C.; van Eldik, R. *Angew. Chem., Int. Ed.* **2008**, *47*, 5238.

(16) Espenson, J. H. *Chemical Kinetics and Reaction Mechanisms*, 2nd ed.; McGraw-Hill: New York, 1995.

(17) Hansch, C.; Leo, A.; Taft, R. W. *Chem. Rev.* **1991**, *91*, 165.

(18) Watanabe, Y.; Iyanagi, T.; Oae, S. *Tetrahedron Lett.* **1980**, *21*, 3685.

(19) Sivasubramanian, V. K.; Ganesan, M.; Rajagopal, S.; Ramaraj, R. *J. Org. Chem.* **2002**, *67*, 1506.

(20) Sastri, C. V.; Seo, M. S.; Park, M. J.; Kim, K. M.; Nam, W. *Chem. Commun.* **2005**, 1405.

(21) Dunford, H. B. *Heme Peroxidases*; Wiley-VCH: New York, 1999.

(22) Collins, T. J.; Khetan, S. K.; Ryabov, A. D. In *Handbook of Green Chemistry*; Anastas, P. T., Crabtree, R. H., Eds.; Wiley-VCH: Weinheim, Germany, 2009; pp 39−77.